Journal of Mathematical Chemistry, Vol. 39, Nos. 3/4, May 2006 (© 2006)
DOI: 10.1007/s10910-005-9042-0

The enhancement of efficiency of high-order harmonic in intense laser field based on asymptotic boundary conditions and symplectic algorithm

Chunli Zhang, Xueshen Liu,* Peizhu Ding

Institute of Atomic and Molecular Physics, Jilin University, Changchun 130012, People's Republic of China
E-mail: liuxs@jlu.edu.cn

Yueying Qi

Institute of Atomic and Molecular Physics, Jilin University, Changchun 130012, People's Republic of China
School of Electrical Engineering, Jiaxing University, Jiaxing 314001, People's Republic of China

Received 28 September 2005; revised 11 October 2005 / Published online: 4 January 2006

Asymptotic boundary condition (ABC) of laser-atom interaction presented recently is applied to transform the initial value problem of the time-dependent Schrödinger equation (TDSE) in infinite space into the initial and boundary value problem in the finite space, and then the TDSE is discretized into linear canonical equations by substituting the symmetry difference quotient for the 2-order partial derivative. The canonical equation is solved by symplectic algorithm. The ground state and the equal weight coherent superposition of the ground state and the first excited state have been taken as the initial conditions, respectively, while we calculate the population of bound states, the evolution of average distance and the high-order harmonic generation (HHG). The conversion efficiency of HHG can be enhanced by initial coherent superposition state and moderate laser intensities.

KEY WORDS: asymptotic boundary condition, symplectic algorithm, high-order harmonic generation, superposition state

1. Introduction

When an atom is exposed to an intense laser field, it emits high-order harmonics via nonlinear interaction of the electrons with the intense radiation field and the ion core. High order harmonic generation (HHG) has been widely studied in strong field physics, and is well explained by the three-step model [1]. The maximum harmonic order of cut-off is $N_m = (I_p + 3.17U_p)/\omega$ [2], where I_p

*Corresponding author.

is the ionization potential, U_p is the ponderomotive energy of the free electron in the electromagnetic field, ω is the frequency of the laser field. As the useful of the HHG the effort of enhancing conversion efficiency and expanding the plateau hasn't been stopped. It is well known that the traditional perturbation theory is invalid to describe the laser-atom interaction in the intense laser field when the intensity of the laser field is greater than 10^{13} W/cm^2. So people look for non-perturbation method, in which the numerical method is used, to solve the time-dependent Schrödinger equation (TDSE) [3–7]. But the problem of the boundary where has been truncated in the numerical calculation has to be considered since the numerical calculation can not to infinite space. Owing to the complexity of an atom in the laser field, the artificial boundary conditions, e.g. an absorber [8] or a mask function [9], are often applied to compute the TDSE so as to eliminate the reflection of the wave-function on the boundaries.

In this paper the asymptotic boundary condition (ABC) of laser-atom interaction presented recently [10–11] is reviewed; the reasonable of ABC is illustrated; the TDSE is solved by using symplectic algorithm which is a difference method that preserves the symplectic structure and a better method on the long-time many-step calculation; and population of bound states, the evolution of average distance and HHG are evaluated. We also show that the conversion efficiency of HHG can be enhanced by taking the equal weight coherent superposition of the ground state and the first excited state as initial condition with the moderate laser intensities. Finally we give the explanation by using the three-step theory.

2. Asymptotic boundary condition

It is shown that one-dimensional model is a good approximation in considering the interaction of intense linearly polarized laser with atom [12]. Under the length gauges and electric-dipole approximation the one-dimensional TESD of model atom in the intense laser field can be written as follows (the atomic units are used in this paper)

$$i\frac{\partial}{\partial t}\Psi(x,t) = \left[-\frac{1}{2}\frac{\partial^2}{\partial x^2} + V_0(x) + \varepsilon(t)x\right]\Psi(x,t), \quad (t \geqslant 0, -\infty < x < \infty) \quad (1)$$

$$\Psi(x,0) = \Phi(x) \quad (-\infty < x < \infty) \quad (2)$$

$$\int_{-\infty}^{\infty} |\Psi(x,t)|^2 dx = 1 \quad (t \geqslant 0, -\infty < x < \infty), \quad (3)$$

where $V_0(x)$ is the atomic potential and $\varepsilon(t)$ is the electric field of the laser pulse, $\Phi(x)$ is the initial wave function. We consider the short-rang model Pöschl–Teller potential which is given by

$$V_0(x) = -\frac{U_0}{\cosh^2(\alpha x)}.$$

If we choose α=0.4 and U_0=0.7, there are three bound states for this short-rang potential, and corresponding eigenfunctions are

$$\varphi_0(x) = \tfrac{4}{\sqrt{15\pi}}(\cosh(\alpha_0 x))^{-2.5},$$
$$\varphi_1(x) = \tfrac{4}{\sqrt{5\pi}}(\cosh(\alpha_0 x))^{-1.5}\tanh(\alpha_0 x),$$
$$\varphi_2(x) = \sqrt{\tfrac{6}{5\pi}}[(\cosh(\alpha_0 x))^{-0.5} - \tfrac{4}{3}(\cosh(\alpha_0 x))^{-2.5}],$$

eigenvalues are $E_0 = -0.5$ a.u., $E_1 = -0.18$ a.u., $E_2 = -0.02$ a.u., respectively. The laser field was chosen to be

$$\varepsilon(t) = \begin{cases} \varepsilon_0 \sin^2\left(\dfrac{\omega_0 t}{2N}\right)\sin(\omega_0 t) & (t_{\text{on}} \leqslant t \leqslant NT_0), \\ 0 & (NT_0 \leqslant t \leqslant t_{\text{off}}), \end{cases}$$

where ε_0 is the peak amplitude of the laser field, ω_0 is the frequency of laser field and $f(t) = \sin^2(\omega_0 t/2N)$ is the pulse envelop, N is the number of optics period, and $T_0 = 2\pi/\omega_0$ is the optical period.

To solve equation (1) numerically, the infinite space has to be truncated into a finite space. Figure 1(a) shows the evolution of total potential energy $(V_0(x) + \varepsilon(t)x)$, figure 1(b) shows the evolution of potential energy when $\varepsilon(t) = \varepsilon_0 = 0.05$ a.u. Figure 1 reveals that the localized potential of atom has been distorted so that the electron can tunnel, which means that the electron has the probability at large distance. Thus the values of the wave functions at the finite boundary can't be simply taken as zero. Compared with the laser field, the effect of the atom potential can be neglected at sufficiently large distance R, which is because the atom potential is monotonously attenuation with the increase of $|x|$. Figure 1 shows that at the large distance R the effect of the laser field is dominated, thus we can neglect $V_0(x)$ when $|x| \geqslant R$, the equation (1) becomes

$$\begin{cases} i\dfrac{\partial}{\partial t}\tilde{\Psi}(x,t) = \left[-\tfrac{1}{2}\dfrac{\partial^2}{\partial x^2} + \varepsilon(t)x\right]\tilde{\Psi}(x,t) & (t \geqslant 0, |x| \geqslant R), \\ i\dfrac{\partial}{\partial t}\Psi(x,t) = \left[-\tfrac{1}{2}\dfrac{\partial^2}{\partial x^2} + V_0(x) + \varepsilon(t)x\right]\Psi(x,t) & (t \geqslant 0, |x| < R). \end{cases} \tag{1'}$$

The following equation (1)″ has the same solution as the equation (1)′ when $|x| \geqslant R$

$$i\frac{\partial}{\partial t}\tilde{\Psi}(x,t) = \left[-\frac{1}{2}\frac{\partial^2}{\partial x^2} + \varepsilon(t)x\right]\tilde{\Psi}(x,t) \quad (t \geqslant 0, -\infty < x < \infty). \tag{1''}$$

We can obtain the solution of equation (1)″ by using Fourier transformation and inverse Fourier transformation [10–11,13]. When $x = \pm R$, the solution $\tilde{\Psi}(x,t)$ of equation (1)″ is

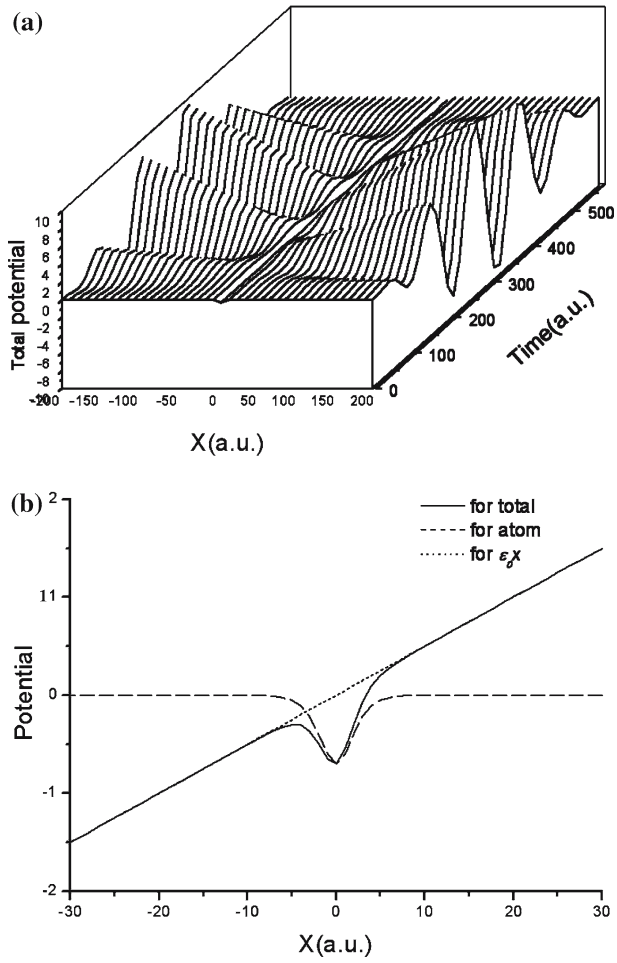

Figure 1. Potential energy of the laser and the atom, $U_0 = 0.7$, $\alpha = 0.4$, $\varepsilon_0 = 0.05$, $\omega_0 = 0.055$, $N = 5$.

$$\tilde{\Psi}(\pm R, t) = \Phi(\pm R - \alpha(t)) \exp\left(-iA(t)(\pm R) - i\frac{1}{2}q(t)\right), \tag{4}$$

where $A(t) = -\int_0^t \varepsilon(t')\mathrm{d}t'$ is the vector potential, $\alpha(t) = -\int_0^t A(t')\mathrm{d}t'$ and $q(t) = \int_0^t A^2(t')\mathrm{d}t'$. We can take equation (4) as the boundary condition of equation (1) at $x = \pm R$, i.e.

$$\Psi(\pm R, t) = \tilde{\Psi}(\pm R, t). \tag{5}$$

This is called the asymptotic boundary condition (ABC). Thus equation (1) can be solved numerically in the finite domain $[-R, R]$ by using the ABC.

Now let's analyze the reasonable of ABC. What we are concerned about is the population of the wave-function at the boundaries $x = \pm R$. We note that $|\tilde{\Psi}(\pm R, t)|^2 = |\Phi(\pm R - \alpha(t))|^2$ from equation (4), namely, the population of ABC at $(\pm R)$ is equal to the population of initial wave-function at $(\pm R - \alpha(t))$. Figure 2 exhibits the evolution of $\alpha(t)$ in the duration of pulse. Taking the population of left boundary as example, because of $|\tilde{\Psi}(-R, t)|^2 = |\Phi(-R - \alpha(t))|^2$ and $\Phi(x) = 0$ when $|x| \geqslant R$, the value of $|\Phi(-R - \alpha(t))|^2$ is zero when $\alpha(t) \geqslant 0$ which is equal to the zero boundary condition; but the value of $|\Phi(-R - \alpha(t))|^2$ is greater than zero when $\alpha(t) < 0$, where the ABC can't be neglected and plays an important role at the points a, b, c, d of figure 2.

3. Numerical recipe

If we let

$$\Psi(x, t) = a(x, t) + ib(x, t), \qquad V(x, t) = V_0(x) + \varepsilon(t)x \tag{6}$$

and divide the whole space $[-R, R]$ into $2N$ equal segments, where N is a sufficiently large positive integer,

$$\tilde{\Psi}(-R) = a_{-N} + ib_{-N}, \qquad \tilde{\Psi}(R) = a_N + ib_N \tag{7}$$

substitute the symmetry difference quotient for the 2-order partial derivative $\dfrac{\partial^2 \Psi_j}{\partial x^2} = \dfrac{\Psi_{j-1} - 2\Psi_j + \Psi_{j+1}}{h^2}$, $j = -N+1, \ldots, N-1$, $\Psi_j = \Psi(x_j), V_j = V(x_j, t)$, $x_j = jh$, $h = R/N$, we can discrete the equation (1) into $(2N-1)$-dimensional linear canonical equation as follows

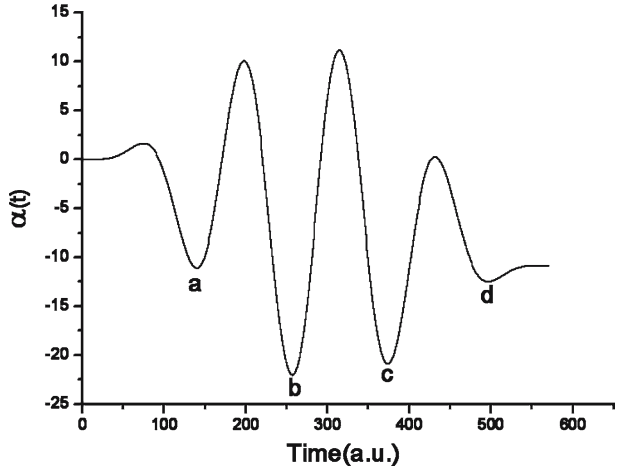

Figure 2. The evolution of $\alpha(t)$ with the same parameters as figure 1.

$$\begin{cases} \dot{b}_j = -\dfrac{1}{2h^2}\{a_{j-1} + [-2 - 2h^2 V_j]a_j + a_{j+1}\} \\ \dot{a}_j = \dfrac{1}{2h^2}\{b_{j-1} + [-2 - 2h^2 V_j]b_j + b_{j+1}\} \end{cases} \quad (j = -N+1, \ldots, N-1). \tag{8}$$

The Hamiltonian function is $H(a_j, b_j, t) = \sum_{j=-N+1}^{N-1} (H_{a_j} + H_{b_j})$, where

$$\begin{cases} H_{a_j} = -\dfrac{1}{2h^2}\{a_{j-1}a_j + [-1 - h^2 V_j]a_j^2 + a_{j+1}a_j\} \\ H_{b_j} = \dfrac{1}{2h^2}\{b_{j-1}b_j + [-1 - h^2 V_j]b_j^2 + b_{j+1}b_j\} \end{cases} \quad (j = -N+1, \ldots, N-1). \tag{9}$$

Let $A = (a_{-N+1}, \ldots, a_{N-1})^T$, $B = (b_{-N+1}, \ldots, b_{N-1})^T$, $Y_1 = (1/2h^2) \times (a_{-N}, 0, \ldots, 0, a_N)^T$, $Y_2 = (1/2h^2) \times (b_{-N}, 0, \ldots, 0, b_N)^T$,

$$S(t) = \frac{1}{2h^2} \begin{pmatrix} -2 - 2h^2 V_{-N+1} & 1 & & & 0 \\ & \vdots & & & \\ & 1 & -2 - 2h^2 V_j & 1 & \\ & & & \vdots & \\ 0 & & & 1 & -2 - 2h^2 V_{N-1} \end{pmatrix}.$$

Equation (8) can be rewritten as

$$\begin{cases} \dot{B} = -SA - Y_1 \\ \dot{A} = SB + Y_2 \end{cases} \tag{10}$$

and the Hamiltonian function is

$$\begin{aligned} H(B, A, t) &= \tfrac{1}{2} B^T S B + Y_2^T B + \tfrac{1}{2} A^T S A + Y_1^T A \\ &= H_1(B, t) + H_2(A, t). \end{aligned}$$

This is a separate Hamiltonian system including explicitly time variable, the symplectic method is a reasonable method to solve canonical equations (10) numerically [11,13–16]. For example, the following 4-stage 4th-order explicit symplectic scheme can be used to solve it.

$$\begin{aligned} &p_1 = B^n - c_1 \tau \left(\frac{\partial H_2(A,t)}{\partial A}\right)_{(A^n, t^n)}, && q_1 = A^n + d_1 \tau \left(\frac{\partial H_1(B,t)}{\partial B}\right)_{(p_1, \zeta_1)}, \\ &\zeta_1 = t^n + c_1 \tau, && \xi_1 = t^n + d_1 \tau; \\ &p_2 = p_1 - c_2 \tau \left(\frac{\partial H_2(A,t)}{\partial A}\right)_{(q_1, \xi_1)}, && q_2 = q_1 + d_2 \tau \left(\frac{\partial H_1(B,t)}{\partial B}\right)_{(p_2, \zeta_2)}, \\ &\zeta_2 = \zeta_1 + c_2 \tau, && \xi_2 = \xi_1 + d_2 \tau; \end{aligned}$$

$$p_3 = p_2 - c_3\tau\left(\frac{\partial H_2(A,t)}{\partial A}\right)_{(q_2,\xi_2)}, \qquad q_3 = q_2 + d_3\tau\left(\frac{\partial H_1(B,t)}{\partial B}\right)_{(p_3,\zeta_3)},$$
$$\zeta_3 = \zeta_2 + c_3\tau, \qquad \xi_3 = \xi_2 + d_3\tau;$$
$$B^{n+1} = p_3 - c_4\tau\left(\frac{\partial H_2(A,t)}{\partial A}\right)_{(q_3,\xi_3)}, \qquad A^{n+1} = q_3 + d_4\tau\left(\frac{\partial H_1(B,t)}{\partial B}\right)_{(B^{n+1},\zeta_4)},$$
$$\zeta_4 = \zeta_3 + c_4\tau = t^{n+1}, \qquad \xi_4 = \xi_3 + d_4\tau = t^{n+1},$$

where $p_j, q_j, \xi_j, \zeta_j,\ j = 1, 2, 3, 4$ are intermediate stages, τ is the time step and

$$c_1 = 0, \quad c_2 = c_4 = \alpha, \quad c_3 = \beta, \quad d_1 = d_4 = \alpha/2, \quad d_2 = d_3 = (\alpha + \beta)/2,$$

or

$$c_1 = c_4 = \alpha/2, \quad c_2 = c_3 = (\alpha + \beta)/2, \quad d_1 = d_3 = \alpha, \quad d_2 = \beta, \quad d_4 = 0.$$

and $\alpha = (2 - 2^{1/3})^{-1}$, $\beta = 1 - 2\alpha$.

4. Numerical results

4.1. High-order harmonic generation

When an atom is exposed to an intense laser field, it gives rise to strongly nonlinear response such as above threshold ionization (ATI) or the HHG. The HHG is a useful energy source, so people are seeking the method to enhance the conversion efficiency of it. The intensity of HHG is proportional to $|d(\omega)|^2$,

$$|d(\omega)|^2 = \left|\frac{1}{t_1 - t_2}\int_{t_1}^{t_2} \mathrm{d}(t)e^{-i\omega t}\right|^2,$$

where $d(t)$ is the electric-dipole moment, which is given by

$$d(t) = -\int_{-R}^{R} \Psi^*(x,t)\frac{\partial V(x,t)}{\partial x}\Psi(x,t)\mathrm{d}x.$$

The three-step model tells us that the dipole momentum is the results of the transitions from the continuum back to the bound states. Watson et al. had evaluated that coherent superposition of the ground state and an excited state as initial condition can enhance conversion efficiency of HHG [17]. High conversion efficiency and high cut-off frequency of HHG can be achieved if the intensity of the laser pulse is high enough for the interaction of $He^+$with intense laser pulse [18].

To investigate the enhancement of conversion efficiency of HHG for the interaction of Pöschl-Teller short-range model potential with intense laser pulse, the ground state and the equal weight coherent superposition of the ground state and the first excited state are considered as the initial input in this paper. In order to illustrate conveniently we denote:

Initial condition I. Take the ground state as the initial condition.

Initial condition II. Take the equal weight coherent superposition of the ground state and the first excited state as the initial condition.

The parameters are chosen as follows: The sufficiently large distance $R = 200$ a.u., the frequency $\omega_0 = 0.055$ a.u., and $N = 5, U_0 = 0.7, \alpha = 0.4$ with different laser intensity (0.01a.u., 0.03a.u., 0.05a.u.).

(1) $\varepsilon_0 = 0.01$ a.u. (0.35×10^{15} W/cm^2)

Figure 3 shows the population of three bound states and spectrum of HHG with different initial input for $\varepsilon_0 = 0.01$ a.u. Figure 3(a) and (b) depict the evolution of the population of three bound states with initial condition I and initial condition II, respectively; figure 3(c) depicts the spectrum of HHG for different initial input. We note that the changes of the population with initial condition I are not distinct, but the populations of the ground state and the first excited state have a little changes with initial condition II, which leads to the enhancement of the conversion efficiency of HHG about 9 orders of magnitude as depicted in figure 3(c). But the population of ionization only reaches approximately to 0.003 in figure 3(d). Since the population

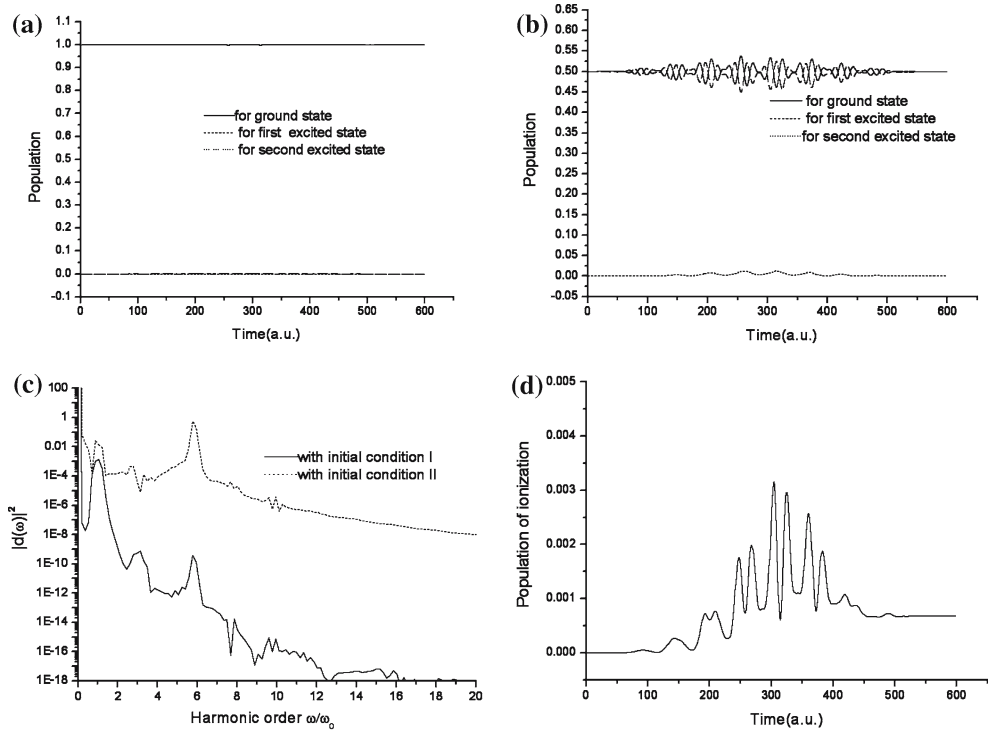

Figure 3. (a) The population of three bound states with initial I; (b) The population of three bound states with initial condition II; (c) The spectrum of harmonic for initial condition I (solid line) and initial condition II (dash line), respectively; and (d) The population of the ionization with initial condition II ($\varepsilon_0 = 0.01$).

of ionization is little in both cases, the characteristic of plateau and the position of cut-off depicted in figure 3(c) is not clear [19].

(2) $\varepsilon_0 = 0.03$ a.u. (1.05×10^{15} W/cm^2)

The numerical results are shown in figure 4 when the intensity of laser pulse is increased to 0.03 a.u., figure 4(a) indicates that the changes of the population of three bound states are small with the initial condition I, so a little electron is radiated to the continuum; figure 4(b) illustrates that the population of ground state and second excited state oscillate about 0.5 and 0, respectively, with the initial condition II, the minimum of population of first excited state reaches approximately to 0.05. Figure 4(d) tells us that the maximum population of ionization reaches approximately to 0.44. We can see that the result of initial condition II enhances the conversion efficiency of HHG about 5 orders of magnitude as depicted in figure 4(c) and the characteristic of HHG in both cases are clear.

(3) $\varepsilon_0 = 0.05$ a.u.(1.75×10^{15} W/cm^2)

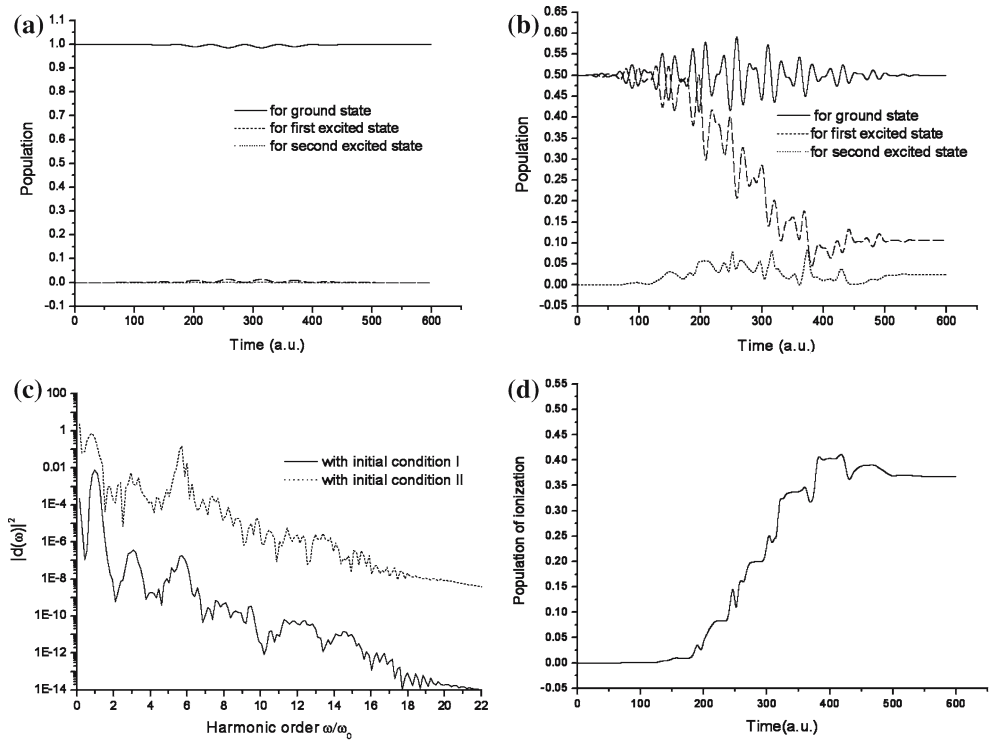

Figure 4. (a) The population of three bound states with initial condition I; (b) The population of three bound states with initial condition II; (c) The spectrum of harmonic with the initial condition I (solid line) and the initial condition II (dot line) respectively and (d) The population of the ionization with initial condition II ($\varepsilon_0 = 0.03$).

The numerical results are shown in figure 5 when the intensity of laser field increased to 0.05 a.u. Figure 5(a) reveals that the changes of three bound states are more obvious than that of in the Figure 4(a) with the initial condition I; figure 5(b) indicates that the population of ground state and second excited state oscillate about 0.5 and 0, respectively, with the initial condition II. Figure 5 (d) tells us that the maximum population of ionization reaches approximately to 0.50, while velocity of ionization of the first excited state is faster than that case of figure 4(d). The enhancement of plateau is about 3 orders of magnitude and cut-off frequency extends to about 23rd.

4.2. *The average distance*

To explain the enhancement of the conversion efficiency of HHG, we calculate the average distance of electron which is given by

$$\bar{x}(t) = \langle \Psi(x,t)|x|\Psi(x,t)\rangle.$$

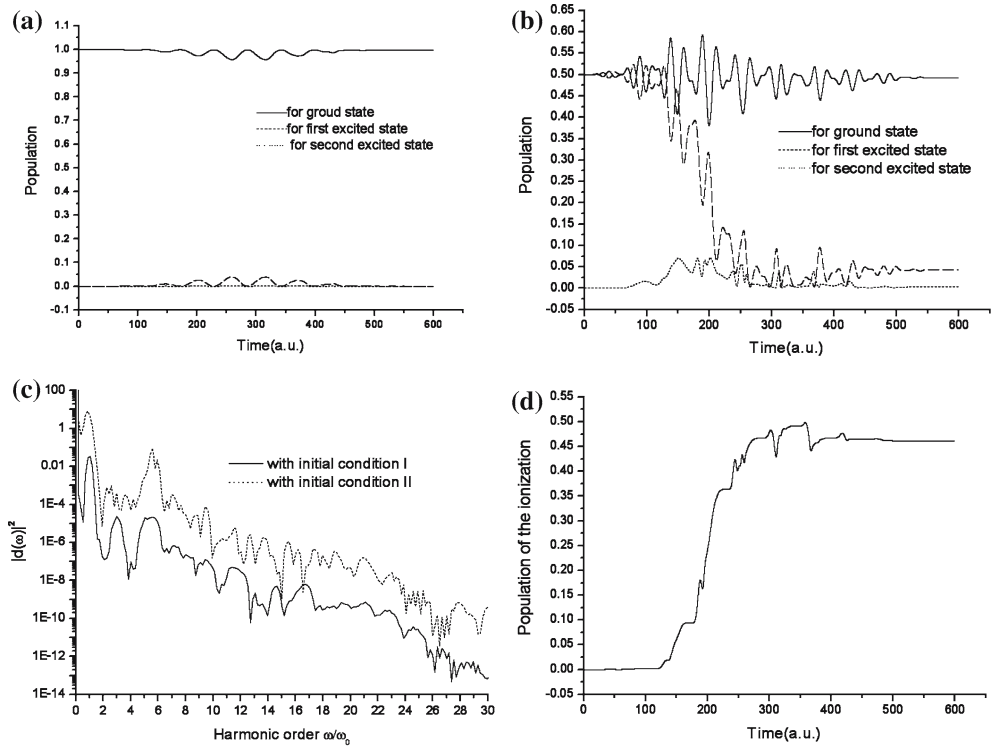

Figure 5. (a) The population of three bound states with the initial condition I; (b) The population of three bound states with the initial condition II; (c) The spectrum of harmonic with the initial condition I (solid line) and the initial condition II (dot line), respectively; and (d) The population of ionization with the initial condition II ($\varepsilon_0 = 0.05$).

Figure 6 shows the evolution of average distance of electron with time in the laser field for different initial conditions. In figure 6, the solid line is for initial condition I and the dot line is for initial condition II. The maximum of average distance and the vibration frequency is increased for initial condition II, which leads to increase the probability of re-collision of electron with ion core so that more high-energy photons can be radiated back to bound states and the conversion efficiency of HHG can be enhanced. But there are different with initial condition II in three pictures of figure 6: the electron vibrates near the core in figure 6(a), but the electron is difficult to return and re-collision with ion core while the intensities of laser field is increased in figure 6(b) and (c). This can explain that the orders of enhancement of conversion efficiency are falling from about 9 to about 3 orders of magnitude when intensity is increased. Namely, to obtain the high conversion efficiency, it is requested that the electron vibrates quickly and can return back to bound states and recombines with core.

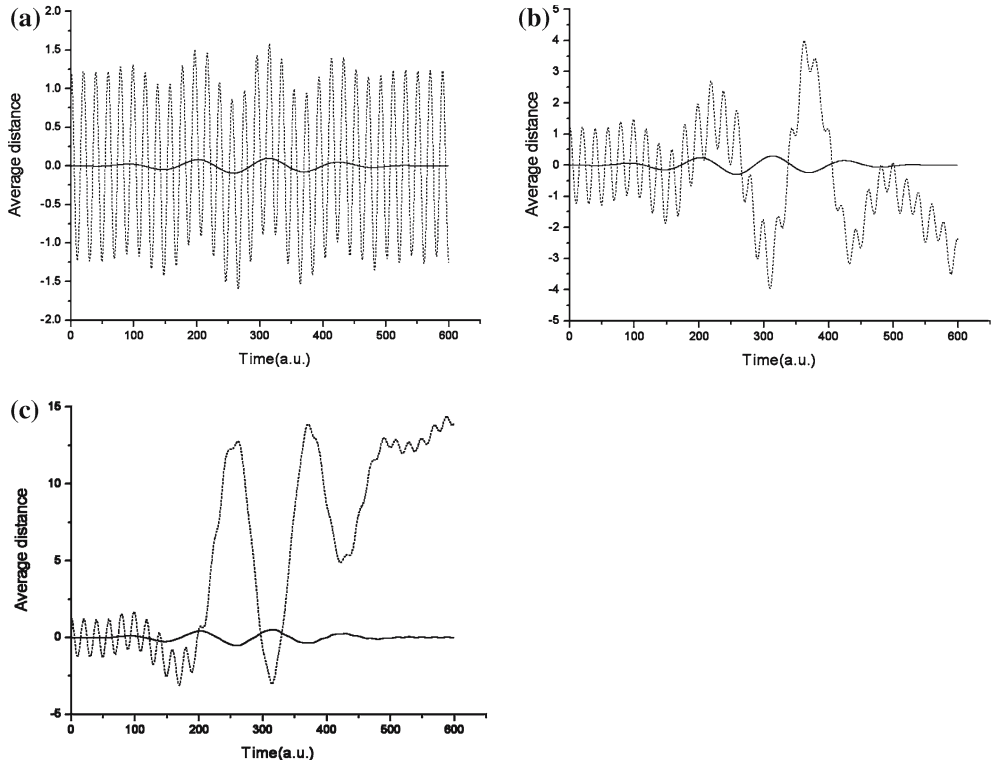

Figure 6. The evolutions of the average distance with initial condition I (solid line) and with the initial condition II (dot line). (*a*) $\varepsilon_0 = 0.01$, (*b*) $\varepsilon_0 = 0.03$, (*c*) $\varepsilon_0 = 0.05$.

5. Discussions

We have reviewed the ABC presented recently and illustrated that the ABC is reasonable for describing the interaction of laser-atom. We solved the 1-D TDSE of interaction between laser and atom by symplectic schemes. The populations of bound states, HHG and the evolution of average distance have been demonstrated by two initial conditions for different laser intensities. The conversion efficiency of HHG can be enhanced when the initial condition II was used. According to the three-step model, the cause of HHG is that the high-energy photons are emitted while electron returns to bound states from the continuum, namely the transition between the continuum and the bound states. Based on the selection rule of transition, the channels of the transition from the bound states to the odd parity and even parity continuum are unobstructed when the initial condition II was used, which afford the possibility of radiating more high-energy photons and enhance the conversion efficiency of HHG; Simultaneity the moderate laser intensities were chosen to insure that some population of electron is being at the continuum and the electron can return back to the bound states as much as possible.

Acknowledgments

This work was supported by The National Natural Science Foundation of China (10574057, 10571074, 10171039), 985 Project of the Ministry of Education of China and The Young Teacher Foundation of Jilin University.

References

[1] C.F.M. Faria and I. Rotter, Phys. Rev. A 66 (2002) 013402.
[2] J.L. Krause, K.J. Schafer and K.C. Kulander, Phys. Rev. Lett. 68 (1992) 3535–3538.
[3] B.I. Schneider, Phys. Rev. A 55 (1997) 3417–3421.
[4] K. Burnett, V.C. Reed, J. Cooper and P.L. Knight, Phys. Rev. A 45 (1992) 3347–3349.
[5] K.C. Kulander, Phys. Rev. A 35 (1987) 445–447.
[6] V. Véniard, R. Taïeb and A. Maquet, Phys. Rev. A 65 (2001) 013202.
[7] H.X. Qiao and B.W. Li, Nucl. Phys. Rev. (in Chinese) 19 (2002) 257–260.
[8] J.L. Krause, K.J. Schafer and K.C. Kulander, Phys. Rev. A 45 (1992) 4998–5010.
[9] S.X. Hu and Z.Z. Xu, Phys. Rev. A 56 (1997) 3916–3922.
[10] X.S. Liu, Y.Y. Qi, W. Hua and P.Z. Ding, Progr. Nat. Sci. 14(7) (2004) 573–581.
[11] Y.Y. Qi, X.S. Liu, X.Y. Liu and P.Z. Ding, J. Math. Chem. (2005) DOI: 10.1007/s10910-005-9009-1.
[12] K.J. LaGattuta, J. Opt. Soc. Am. B10(5) (1993) 958–962.
[13] X.Y. Liu, X.S. Liu, P.Z. Ding and Z.Y. Zhou, The symplectic algorithm for use in a model of laser field, X-Ray Lasers: 8th International Conference on X-Ray Lasers, (2002) 265–270.
[14] K. Feng, J. Comput. Math. 4(3) (1986) 279–289.
[15] Y.Y. Qi, X.S. Liu and P.Z. Ding, Int. J. Quant. Chem. 101 (2005) 21–26.

[16] Th. Monovasilis and T.E. Simos, Chem. Phys. 313 (2005) 293–298.
[17] J.B. Watson, A. Sanpera, X. Chen and K. Burnett, Phys. Rev. A 53 (1996) R1962–R1965.
[18] B.B. Wang, T.W. Cheng, X.F. Li and P.M. Fu, Chin. Phys. Lett. 21 (2004) 1727–1729.
[19] M. Protopapas, C.H. Keitel and P.L. Knight, Rep. Prog. Phys. 60 (1997) 389–486.